Fourth Australia - New Zealand
Conference on Geomechanics,
Perth, 14-18 May 1984

The Dilatancy of Sand Under a General Stress System

M.S. MESDARY
Director, Road Research Centre, Ministry of Public Works, Kuwait

SUMMARY:- A general form of the stress-dilatancy equation is derived which applies to the special cases of axial symmetry as derived by Rowe (1962) and Rowe, Barden and Lee (1964), plane strain as derived by Rowe (1964), and in any case in which the effective intermediate principal stress σ'_2 varies between the effective major principal stress σ'_1 and the effective minor principal stress σ'_3.

Experimental results showed that the effective stress ratio σ'_1/σ'_3 up to its maximum value was a linear function of the dilatancy, the function being independent of the porosity of the material but dependent on the ratio of two of the principal stresses. The maximum dilatancy was found to be independent of σ'_2, and a relation between the maximum effective stress ratio, the maximum dilatancy and the relative porosity was postulated.

INTRODUCTION

A knowledge of the stress-strain relationship for soils constitutes a fundamental step towards the solution of engineering problems. Because of the random and discrete nature of granular material, it has been difficult to formulate theoretical stress-strain relationship which govern their behaviour and thus elastic or plastic models have been generally adopted in order to solve soil engineering problems. In these two approaches the discrete nature of granular materials is not considered; hence actual stress-strain relations for soil are needed. Rowe (1962) adopted an approach in which the discrete nature of granular material was considered and the stress-dilatancy equation was found to be given by:

$$\sigma'_1/\sigma'_3 = \left(1 - \frac{\delta dV/V}{\delta\varepsilon_1}\right) \tan^2(45 + \phi\mu/2) \qquad (1)$$

where: σ'_1 = effective major principal stress,
σ'_2 = effective minor principal stress,
dV/V = natural volumetric strain,
ε_1 = natural major principal strain,
$\phi\mu$ = true angle of friction between grains.

Tests were conducted by Rowe (1962) in the triaxial compression apparatus and agreement with equation (1) was found for the case of dense soils. In the case of loose, normally consolidated soils, the stress ratio σ'_1/σ'_3 was found to be greater than that given by equation (1), and thus to allow for the excess energy absorbed, Rowe (1962) modified equation (1) to:

$$\sigma'_1/\sigma'_3 = \left(1 - \frac{\delta dV/V}{\delta\varepsilon_1}\right) \tan^2(45 + \phi_f/2) \qquad (2)$$

where ϕ_f = modified angle of interparticle friction which fits the observation.

Tests conducted in the triaxial apparatus show good agreement with equation (2) for dense, medium dense and loose soils with $\phi_f = \phi\mu$, Lee (1966), Barden and Khayatt (1966), and Khayatt and Wightman (1969). For the case of plane strain, Rowe (1964), Rowe (1969) and Barden et al (1969) found that for any density there was good agreement with equation (2) with $\phi_f = \phi\mu$, the coulomb angle of shearing resistance at the state of critical void ratio. Rowe, Barden and Lee (1964) extended the work to cover the case of extension test where $\sigma'_1 = \sigma'_2 > \sigma'_3$, and the stress dilatancy relation was found to be:

$$(\sigma'_1/\sigma'_3)\left(1 - \frac{\delta dV/V}{\delta\varepsilon_3}\right) = \tan^2(45 + \phi_f/2) \qquad (3)$$

where ε_3 = the natural minor principal strain.

From extension tests, Barden and Khayatt (1966) found good agreement with equation (3) for dense and medium sand with $\phi_f = \phi\mu$. An extension of the Stress-Dilatancy Equation for the general case where $\sigma'_1 \neq \sigma'_2 \neq \sigma'_3$ is given in the Appendix.

EXPERIMENTAL INVESTIGATIONS

(1) Apparatus. Sutherland and Mesdary (1969) described an apparatus in which the principal stresses can be varied in any desired manner. They also showed that the sample deformed freely under the applied stresses. A photograph of the apparatus is given in Fig. (1), and in the apparatus, cubical samples of 4-inch sides can be tested under three different principal stresses.

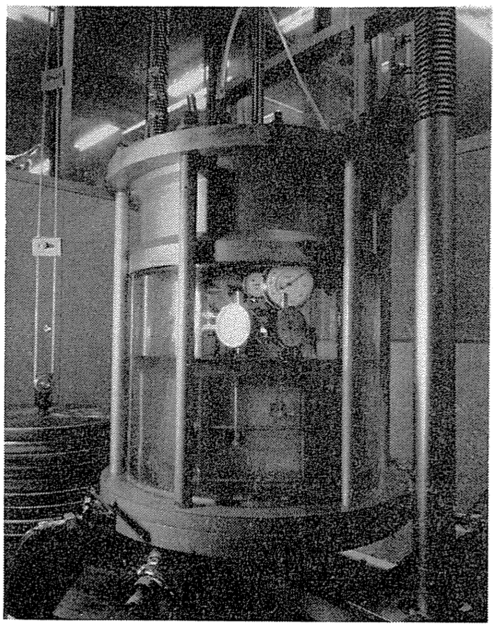

Figure 1

(2) Materials. Two materials were tested; namely, Loch Aline sand and Glass Ballotini grade 12. The grading curves are shown in Fig. (2), and other properties as shown in the table.

	Loch Aline	Glass Ballotini
Specific gravity	2.65	2.94
Uniformity coefficient D_{60}/D_{10}	1.30	1.50
ϕ_μ (after Rowe 1962)	26°-26.30°	17.30°-18°
Porosity limits* n_{max}-n_{min},	0.445-0.349	0.427-0.357

*After J. Kolbuszewski, 1948

(3) Sample Preparation and Test Procedures. Tests were carried out in which samples were subjected to a general stress path where σ_2' was varied between σ_1' and σ_3'. A detailed description of the test procedure was given by Sutherland and Mesdary (1969) for Loch Aline sand and a similar procedure was followed for testing Glass Ballotini.

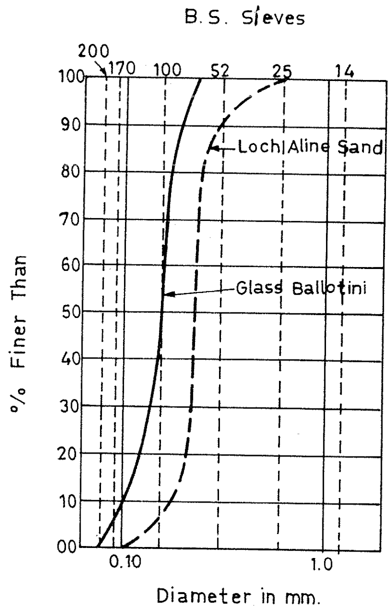

Figure 2

PRESENTATION AND DISCUSSION OF RESULTS

Sutherland and Mesdary (1969) reported representative plots of σ_1'/σ_3' and volumetric strain against the axial natural strain in the vertical direction. Results on Glass Ballotini showed a similar pattern and there was a well defined peak behaviour at which the rate of dilatancy was generally a maximum. The strength of Glass Ballotini, as found for Loch Aline sand, was higher in the case of $\sigma_1' \neq \sigma_2' \neq \sigma_3'$ than in the case of axial symmetry.

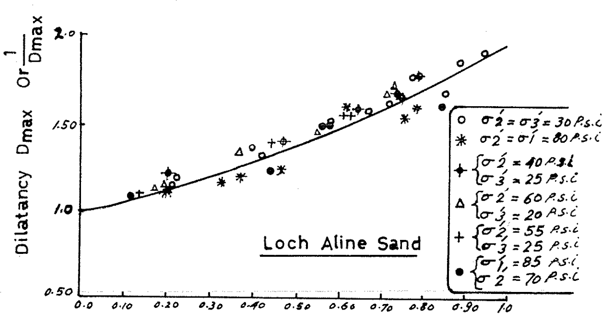

Figure 3

Figure 3 shows the relation between the maximum dilatancy term (see Appendix) D_{max} or $1/D_{max}$ and the initial relative porosity n_r for Loch Aline sand, where:

$$n_r = (n_{max} - n)/(n_{max} - n_{min}) \quad (4)$$

The values of D_{max} correspond to those tests conducted with mean normal stress σ_m' increasing where the values of $1/D_{max}$ correspond to those tests conducted with σ_m' decreasing. The maximum dilatancy generally occured at the peak strength. As shown one can conclude that the maximum dilatancy is independent of σ_2' and the relation between the dilatancy and the relative porosity may be given by:

$$D_{max} = e^{an_r}, \quad \text{for } \sigma_m' \text{ increasing, } (\sigma_z' = \sigma_1' > \sigma_y' = \sigma_2' \geq \sigma_x' = \sigma_3') \quad (5a)$$

or

$$1/D_{max} = e^{an_r}, \quad \text{for } \sigma_m' \text{ decreasing, } (\sigma_y' = \sigma_1' \geq \sigma_x' = \sigma_2' > \sigma_z' = \sigma_3') \quad (5b)$$

where $a = 0.68$ and $e = 2.71828..$,

therefore $$D_{max} = e^{0.68n_r} \quad (5c)$$

or $$1/D_{max} = e^{0.68n_r} \quad (5d)$$

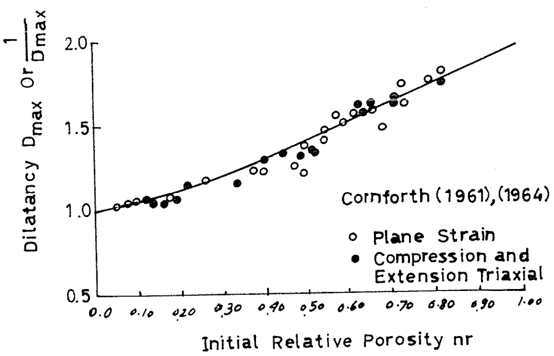

Fig. 4

Fig. 4 shows the results of Cornforth (1964) conducted on Brasted sand under plane strain and axial symmetry, whether extension or compression. Fig. 5 shows the results reported by Barden (1969) and Barden et al (1969) on Welland sand, also under

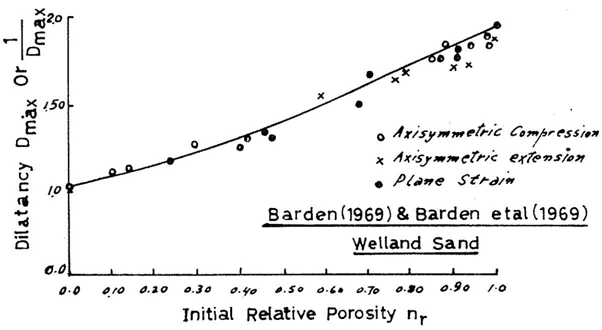

Fig. 5

plane strain and axial symmetrical conditions. The results shown in Figs. 4 and 5 are those given by the previous authors, but after being prepared in the form of Fig. 3.

The results in Figs. 4 and 5 show good agreement with equations (5c) and (5d) and support the finding that the maximum dilatancy is independent of σ_2' for the same mean normal stress.

Fig. 6 shows the relation between D_{max} (or $1/D_{max}$) and n_r for Glass Ballotini. The results show also that D_{max} (or $1/D_{max}$) is independent of σ_2', though a different relation than that given by equations (5c) and (5d) is found. The relations are linear:

$$D_{max} = n_r + 1.10, \quad \sigma_m' \text{ increasing,} \quad (6a)$$

and $$1/D_{max} = n_r + 1.10, \sigma_m' \text{ decreasing.} \quad (6b)$$

The difference in form between equations (5a) and (5b) and equations (6a) and (6b) may be attributed to the difference in the shape of particle contacts for sand and glass balls.

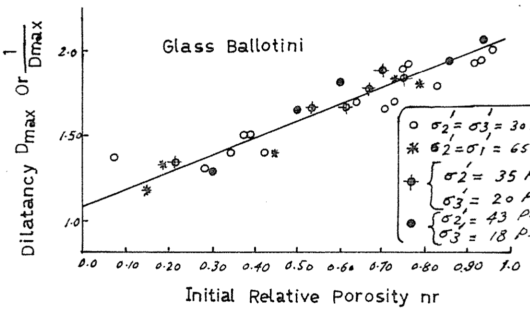

Fig. 6

STRESS-DILATANCY RELATIONSHIPS

Equations A12 and A12' (see Appendix) were derived for the condition of minimum energy. The results were plotted in the form σ_1'/σ_3' against D for tests with σ_m' increasing and against 1/D for tests with σ_m' decreasing. Some typical plots are shown in Figs. 7 to 9 for Loch Aline sand. Similar results were found for Glass Ballotini.

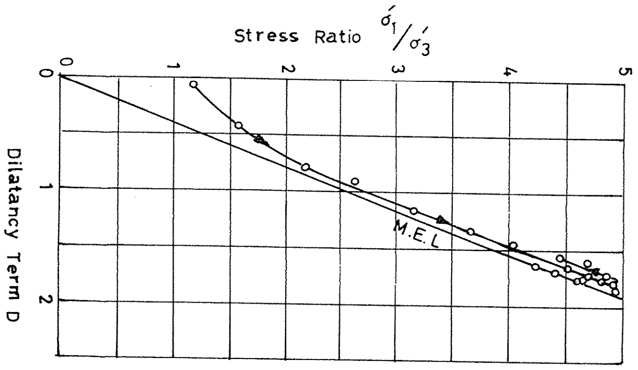

Fig. 7, $\sigma_y' = \sigma_x' = 30$psi, n=0.359

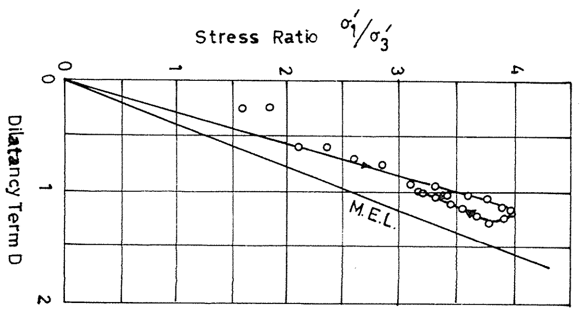

Fig. 8, $\sigma_y' = 60$psi, $\sigma_x' = 20$psi, n= 0.428

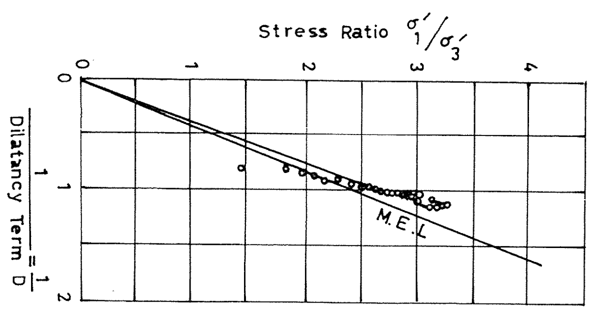

Fig. 9, $\sigma_y' = \sigma_x' = 80$psi, n=0.425

The plots indicated a linear relationship between σ_1'/σ_3' and D (or 1/D) up to the peak stress ratio.

Then $\sigma_1'/\sigma_3' = \sigma_z'/\sigma_x' = (D)Rp_f$, (7a)

where $\sigma_z' > \sigma_y' \geq \sigma_x'$,

and $\sigma_1'/\sigma_3' = \sigma_y'/\sigma_z' = (1/D)Rp'_f$, (7b)

where $\sigma_z' < \sigma_x' \leq \sigma_y'$.

The values of Rp_f and $R'p_f$ are plotted against the porosity n, as shown in Fig. 10 (for Loch Aline sand), and Fig. 11 (for Glass Ballotini), along with values of Kp_μ and Kp_{cv} where $Kp_{cv} = \tan^2(45+\phi_{cv}/2)$. The ϕ_{cv} values were obtained from tests at large strains in the conventional triaxial apparatus following the procedure given by Sutherland and Mesdary (1969), and were found to be 31°30' for Loch Aline sand, and 23° for the Glass Ballotini.

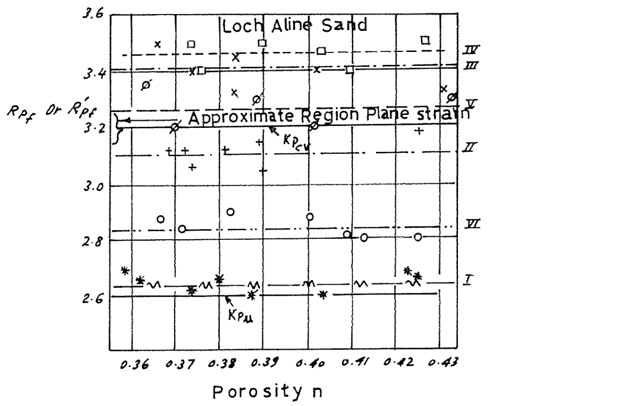

Series I, $\sigma_z' > \sigma_y' = \sigma_x'$, $\sigma_y'/\sigma_x' = 1$
Series II, $\sigma_z' > \sigma_y' > \sigma_x'$, $\sigma_y'/\sigma_x' = 1.60$
Series III, $\sigma_z' > \sigma_y' > \sigma_x'$, $\sigma_y'/\sigma_x' = 2.20$
Series IV, $\sigma_z' > \sigma_y' > \sigma_x'$, $\sigma_y'/\sigma_x' = 3.0$
Series V, $\sigma_z' < \sigma_x' < \sigma_y'$, $\sigma_y'/\sigma_x' = 1.21$
Series VI, $\sigma_z' < \sigma_y' = \sigma_x'$, $\sigma_y'/\sigma_x' = 1.0$

Fig. 10

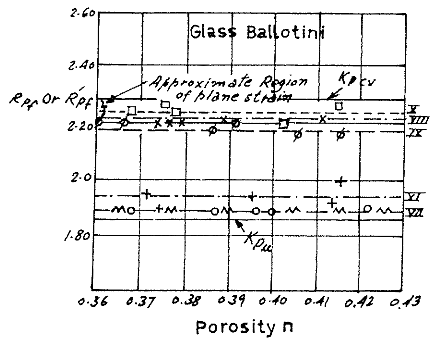

Series VII, $\sigma_z' > \sigma_y' = \sigma_x'$, $\sigma_y'/\sigma_x' = 1.0$
Series VIII, $\sigma_z' > \sigma_y' > \sigma_x'$, $\sigma_y'/\sigma_x' = 1.75$
Series IX, $\sigma_z' > \sigma_y' > \sigma_x'$, $\sigma_y'/\sigma_x' = 2.39$
Series X, $\sigma_z' < \sigma_x' < \sigma_y'$, $\sigma_y'/\sigma_x' = 1.17$
Series XI, $\sigma_z' < \sigma_x' = \sigma_y'$, $\sigma_y'/\sigma_x' = 1.0$

Fig. 11

Figs. 10 and 11 show that the values of Rp_f and $R'p_f$ are practically constant for each of the eleven test series, irrespective of the porosity of the samples over the range of porosities tested.

From equations (7a) and (7b) and equations (5c) and (5d), then at the maximum dilatancy for Loch Aline, Brasted, and Welland sands (which generally occurred at the peak strength):

$$(\sigma_1'/\sigma_3') = Rp_f e^{.68n_r}, \text{ where } \sigma_z' > \sigma_y' \geq \sigma_x', \quad (8a)$$

and $(\sigma_1'/\sigma_3') = R'p_f e^{0.68 n_r}$ (8b)

where $\sigma_y' = \sigma_1' \geq \sigma_x' = \sigma_2' > \sigma_z' = \sigma_3'$,

and from equation (7a) and (7b), equations (6a) and (6b), then for Glass Ballotini:

$$(\sigma_1'/\sigma_3') = (n_r + 1.10)\ Rp_f, \quad (9a)$$

where $\sigma_z' = \sigma_1' > \sigma_y' = \sigma_2' \geq \sigma_x' = \sigma_3'$,

and $$(\sigma_1'/\sigma_3') = (n_r + 1.10)\ R'p_f \quad (9b)$$

where $\sigma_y' = \sigma_1' \geq \sigma_x' = \sigma_2' > \sigma_z' = \sigma_3'$.

The results obtained can be further considered for the cases of axial symmetry and non-symmetry.

(a) Axial Symmetry. For this case, the values of R_{pf} and $R'p_f$ were found to be close to the Kp_μ value, indicating that the energy absorbed was a minimum and that sliding occurred in preferred directions close to the critical β directions. These results found from tests on cubical samples, agree with the findings of previous investigators. Using a Kp_f value, which for axial symmetry should correspond to Rp_f, Rowe (1962), Lee (1966) and Barden and Khayatt (1966), found that Rp_f (Kp_f) was equal to Kp_μ for dense and medium dense soils. Barden et al (1969), have subsequently reported that Rp_f (Kp_f) was equal to Kp_μ for sands tested at different porosities ranging from dense to loose states using cylindrical samples in the triaxial apparatus. For the minimum energy criterion to be followed, samples should have freedom to permit sliding on preferred directions corresponding to the critical β directions. It could be argued that loose samples will have more freedom than dense samples, because of the lesser possibility of particle interlocking. However, the test results indicate that this possibility appears to be of little significance over the wide range of porosities investigated. For very loose materials, erratic particle movements can occur in non-preferred directions because of the instability of the packing and the energy absorbed will then be higher than that of the minimum energy criterion, e.g. Rowe (1962) found ϕ_f to be equal to ϕ_{cv} with very loose soils. However, on reloading the samples, Rowe found that the minimum energy criterion was observed with $\phi_f = \phi_\mu$. Also, Horne (1965) has pointed out that for a very dense material with a high degree of interlocking, the energy absorbed would be greater than that required by the minimum energy criterion, due to the restriction imposed on the particle movements by the high interlocking. Neither extremely loose nor extremely dense materials were used in the present investigation, and within the ranges studied it was found that for the case of axial symmetry the minimum energy criterion was followed.

(b) Non-Symmetry. For this case the values of Rp_f and $R'p_f$ were greater than the Kp_μ value. The energy absorbed was greater than that given by the minimum energy criterion and this shows that sliding occurred on non-preferred directions as discussed by Sutherland and Mesdary (1969). Since the Rp_f and $R'p_f$ values were found to be independent of porosity, it would appear that the restriction on particle movements is due to the applied stress system. For the special case of plane strain, Rowe (1964), Rowe (1969) and Barden et al (1969) found that Rp_f (Kp_f) equalled Kp_{cv}. The Kp_{cv} values for the Loch Aline sand and the Glass Ballotini have been plotted on Figs. 10 and 11 respectively. From the detailed records of the tests, the Rp_f values corresponding to the plane strain condition can be estimated, and these are shown on Figs. 10 and 11. They correspond to the Kp_{cv} values, and are in agreement with the results of the previous investigators.

It is interesting to note that tests conducted by Cole (1967) using the Cambridge Mk.6 S.S.A., in which the sample deformed in simple shear under plane strain conditions showed that Rp_f (Kp_f) is constant for dense and loose sands. Also Rowe (1969) has reported that Proctor (1967) found agreement with equ. (7a&b) for the cases of axial symmetry and plane strain using the hollow cylinder test, with $Rp_f = Kp_\mu$ and $Rp_f = Kp_{cv}$ respectively.

CONCLUSIONS

1. The maximum dilatancy (D_{max} or $1/D_{max}$) is found to be independent of σ_2'. At the maximum dilatancy which generally occured at the peak strength, the stress ratio can be related to the initial relative porosity.

2. The energy absorbed in deforming a sample up to the peak stress ratio was found to be greater for the case of non-symmetry than for axial symmetry.

3. The stress ratio σ_1'/σ_3' up to its maximum value was found to be a linear function of the dilatancy term D or (1/D). The slopes of the lines Rp_f and $R'p_f$ were found to be independent of the porosity of the material and appear to be a function of σ_y'/σ_x'.

REFERENCES

BARDEN, L. and KHAYATT, A.J. (1966). Incremental Strain Rate Ratios And Strength Of Sand in the Triaxial Test. Geotechnique, Vol. 16, No. 4.

BARDEN, L., KHAYATT, A.J. and WIGHTMAN, A. (1969). Elastic And Slip Components Of the Deformation Of Sand. Canadian Geotechnical Journal, 6.

BARDEN, L. (1969). A Quantitative Treatment of the Deformation Behaviour of Granular Material in Terms of Particulate Mechanics., Int. Conf. on Structure, Solid Mechanics And Engineering Design in Civil Engineering Materials, Southampton.

BISHOP, A.W. (1966). The Strength Of Soils as Engineering Materials. Sixth Rankine Lecture, Geotechnique, Vol. 16, No.2.

BISHOP, A.W. and GREEN G.E. (1965). The Influence of End Restraint of the Compression Strength of a Cohesionless Soil. Geotechnique, Vol. 15, No. 3.

COLE, E.R.L. (1967). Soils in the S.S.A. Ph.D. Thesis, Cambridge University.

CORNFORTH, D.H. (1961). Plane Strain Failure Characteristics of a Saturated Sand. Ph.D. Thesis, University of London.

CORNFORTH, D.H. (1964). Some Experiments on the Influence of Strain Conditions on the Strength of Sand. Geotechnique, Vol. 14, No.2.

HORNE, M.R (1965). The Behaviour of an Assembly of Rotund, Rigid, Cohesionless Particles. Proc. Royal Society, A 286.

KOLBUSZEWSKI, J.J, (1948). An Experimental Study of The Maximum And Minimum Porosities of Sands. Proc. 2nd Int. Conf. Soil Mech., Vol. 1.

LEE, I.K. (1966). Stress-Dilatancy Performance of Feldspar. Proc. A.S.C.E., Soil Mech. and Found.

Div., Vol. 92, No.2.

MESDARY, M.S. (1969). The Shearing Behaviour of Granular Material Under a General Stress System. Ph.D. Thesis, University of Glasgow.

PROCTOR, D.C. (1967). The Stress-Dilatancy Behaviour of Dense Sand in the Hollow Cylinder Test. M.Sc. Thesis, Manchester University.

ROWE, P.W. (1962). The Stress-Dilatancy Relation for Static Equilibrium of an Assembly of Particles in Contact. Proc. Royal Society Of London, A 269,

ROWE, P.W. (1964). Correspondence On Some Experiments on the Influence of Strain Conditions on the Strength of Sand by Cornforth, D.H. Geotechnique, Vol. 14, No. 4.

ROWE, P.W. (1969). The Relation Between the Shear Strength of Sands in Triaxial Compression, Plane Strain, and Direct Shear. Geotechnique, Vol. 19, No. 1,

ROWE, P.W., and BARDEN, L. (1964). The Importance of Free Ends in the Triaxial Test. Proc. A.S.C.E., Soil Mech. and Found.Div., Vol. 90, No.1,

ROWE, P.W., BARDEN, L. and LEE, I.K. (1964). Energy Components During the Triaxial Cell and Direct Shear Tests. Geotechnique, Vol. 14, No. 3,

SUTHERLAND, H.B. and MESDARY, M.S. (1969). The Influence of the Intermediate Principal Stress on the Strength of Sand. Proc. 7th Int. Conf. Soil Mech., Vol. 1,

APPENDIX

Consider any two particles in contact, taken from an assembly of particles as shown in Fig. (A1). The axes oz, oy, and ox are taken in the directions of the effective principal stresses to which the assembly of particles are subjected. At any increment of stress, it is also assumed that the directions of the principal strain increments coincide with oz, oy, and ox.

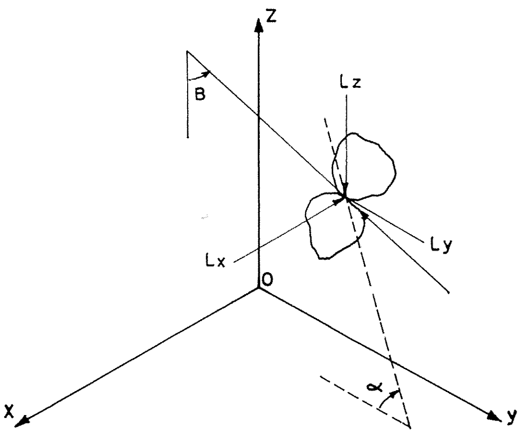

Fig. (A1)

Then, for the two particles in contact, let

L_z, L_y, L_x = the resultant forces acting at the point of contact in the z, y, and x directions, respectively,

A_y, A_z = the areas normal to the y and z directions, respectively,

σ_z', σ_y', σ_x' = the effective principal stresses acting on the assembly in the z, y and x directions,

β = the direction of the sliding contact, measured with respect to the x-z plane as shown in Fig. A1.

Case (1) $\sigma_z' > \sigma_y' \geq \sigma_x'$, (Fig. A2a):

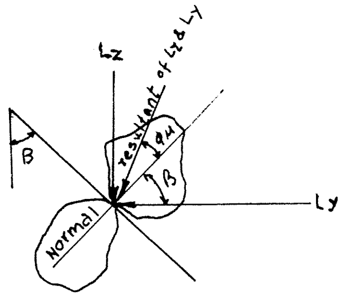

Fig. (A2a)

In a plane parallel to the z-y plane

$$(L_z/L_y) = \tan(\phi_\mu + \beta_{zy}) \tag{A1}$$

and
$$(L_z/L_y)(A_z/A_y) = (\sigma_z'/\sigma_y') = \tan\alpha_{zy}\tan(\phi_\mu + \beta_{zy}) \tag{A2}$$

Similarly, in a plane parallel to the z-x plane,

$$(\sigma_z'/\sigma_x') = \tan\alpha_{zx}\tan(\phi_\mu + \beta_{zx}) \tag{A3}$$

where α and β are the angle of interlocking and the β-angle, respectively, in planes parallel to the planes indicated by suffixes. The suffix zy (or zx) indicates that sliding is occurring in the plane zy (or zx) towards the y (or x) direction.

At any instant of loading, let the volume of an element be denoted by V; thus, during a small increment of loading:

$$\delta dV/V = \delta\varepsilon_z + \delta\varepsilon_y + \delta\varepsilon_x,$$

or
$$\left(1 - \frac{\delta dV/V}{\delta\varepsilon_z}\right) = -(\delta\varepsilon_y/\delta\varepsilon_z) + (\delta\varepsilon_x/\delta\varepsilon_z) \tag{A4}$$

where $\delta\varepsilon_z$, $\delta\varepsilon_y$, $\delta\varepsilon_x$ = increments of the natural strain in the z, y and x directions respectively, and are positive if compressive,

and $\delta dV/V$ = an increment of the natural volumetric strain, and is positive if compressive.

Considering displacements in the z, y and x directions, then during a small increment of loading,

$$-(\delta\varepsilon_y/\delta\varepsilon_z) = k\tan\alpha_{zx}\tan\beta_{zx}, \tag{A5}$$

and
$$-(\delta\varepsilon_y/\delta\varepsilon_z) = (1-k)\tan\alpha_{zy}\tan\beta_{zy}, \tag{A6}$$

where k = a constant during a small increment of stress.

Let δW = an increment of energy absorbed during a small increment of stress,

$$\delta W = \sigma_z'\delta\varepsilon_z + \sigma_y'\delta\varepsilon_y + \sigma_x'\delta\varepsilon_x,$$

then $(\delta W/\sigma_z'\delta\varepsilon_z) = (1 - 1/\delta E)$,

where
$$\delta E = -(\sigma_z'\delta\varepsilon_z/\sigma_y'\delta\varepsilon_y + \sigma_x'\delta\varepsilon_x) \tag{A7}$$
= (Work in/Work out)

From equations (A2), (A3), (A5), and (A6), then,

$$E = -\frac{\tan(\phi_\mu + \beta_{xy})\ \tan(\phi_\mu + \beta_{zx})}{(1-k)\tan\beta_{zy}\tan(\phi_\mu + \beta_{zx}) + k\tan\beta_{zx}\tan(\phi_\mu + \beta_{zy})} \qquad (A8)$$

For the energy absorbed in a small increment of stress to be a minimum, δE should be a minimum.

Hence, $(\partial\delta E/\partial\beta_{zy}) = 0$, and $(\partial\delta E/\partial\beta_{zx}) = 0$,

and from which we find:

$$\beta_{zx} = (45 - \phi_\mu/2) \qquad (A9)$$

and $$\beta_{zy} = (45 - \phi_\mu/2) \qquad (A10)$$

Thus at the critical condition of minimum energy,

$$\beta_{zy} = \beta_{zx} = \beta_{critical} = (45 - \phi_\mu/2) \qquad (A11)$$

and from equations (A2), (A3), (A4), (A5), (A6), and (A11), then.

$$(\sigma'_z/\sigma'_x) = \left(1 - \frac{\delta dV/V}{\delta\varepsilon_z}\right)\left[\frac{1}{k+(1-k)(\sigma'_x/\sigma'_y)}\right]\tan^2(45+\phi_\mu/2),$$

or $$(\sigma'_z/\sigma'_x) = D\chi Kp_\mu \qquad (A12)$$

where $D = \left(1 - \frac{\delta dV/V}{\delta\varepsilon_z}\right)$ is the dilatancy term,

$\chi = 1/[k + (1 - k)(\sigma'_x/\sigma'_y)]$,

and $Kp_\mu = \tan^2(45+\phi_\mu/2)$.

From equations (A2), (A3), (A5), (A6), and (A11) then,

$$k = (\sigma'_x\delta\varepsilon_x)/(\sigma'_x\delta\varepsilon_x + \sigma'_y\delta\varepsilon_y) \qquad (A13)$$

Equations (A11)-(A13) only apply at the critical condition of minimum energy. Equation (A12) is thus a lower bound.

Case (2):

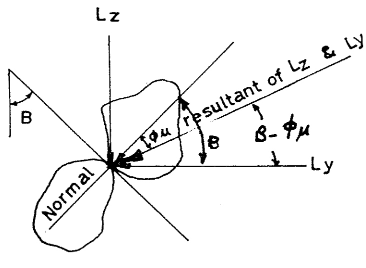

Fig. (A2b)

In a procedure similar to Case 1, the corresponding equations can be written as:

$$(L_z/L_y) = \tan(\beta_{yz}-\phi_\mu) \qquad (A1')$$

and $$(\sigma'_z/\sigma'_y) = \tan\alpha_{yz}\tan(\beta_{yz}-\phi_\mu) \qquad (A2')$$

$$(\sigma'_z/\sigma'_x) = \tan\alpha_{xz}\tan(\beta_{xz}-\phi_\mu) \qquad (A3')$$

$$\left(1 - \frac{\delta dV/V}{\delta\varepsilon_z}\right) = -[(\delta\varepsilon_y/\delta\varepsilon_z)+(\delta\varepsilon_x/\delta\varepsilon_z)] \qquad (A4')$$

$$-(\delta\varepsilon_x/\delta\varepsilon_z) = k\tan\alpha_{xz}\tan\beta_{xz} \qquad (A5')$$

$$-(\delta\varepsilon_y/\delta\varepsilon_z) = (1-k)\tan\alpha_{yz}\tan\beta_{yz} \qquad (A6')$$

Therefore $\delta w = \sigma'_z\delta\varepsilon_z + \sigma'_y\delta\varepsilon_y + \sigma'_x\delta\varepsilon_x$

and $\delta w/\sigma'_z\delta\varepsilon_z = 1-\delta E'$

where $$\delta E' = -(\sigma'_y\delta\varepsilon_y + \sigma'_x\delta\varepsilon_x)/(\sigma'_z\delta\varepsilon_z) \qquad (A7')$$

$$= \text{(Work in)/(Work out)}$$

$$\delta E' = \frac{k\tan\beta_{xz}\tan(\beta_{yz}-\phi_\mu)+(1-k)\tan\beta_{yz}\tan(\beta_{xz}-\phi_\mu)}{\tan(\beta_{yz}-\phi_\mu)\tan(\beta_{xz}-\phi_\mu)}, \qquad (A8')$$

and for the critical condition of minimum energy

$$\beta_{yz} = \beta_{xz} = \beta_{critical} = (45 + \phi_\mu/2) \qquad (A11')$$

Then, $$(\sigma'_x/\sigma'_z) = (1/D)\chi\ Kp_\mu \qquad (A12')$$

$$k = (\sigma'_x\delta\varepsilon_x)/(\sigma'_x\delta\varepsilon_x + \sigma'_y\delta\varepsilon_y) \qquad (A13')$$

where $\chi = k + (1-k)(\sigma'_x/\sigma'_y) = 1/\chi$

and $Kp_\mu = \tan^2(45 + \phi_\mu/2)$

Equations (A11'), (A12'), and (A13') apply only at the critical condition of minimum energy when sliding occurs at the critical β-angle.

It is interesting to note that, since sliding is occurring in the opposite direction to that given in case (1), Equations (A11') and (A12') may be obtained from Equations (A11) and (A12) by substituting ϕ_μ with $(-\phi_\mu)$.

Special Cases

(a) The Case of Axial Symmetry, where $\sigma'_z > \sigma'_y = \sigma'_x$

This is the case of the triaxial compression test. Thus $\sigma'_z=\sigma'_1, \sigma'_y=\sigma'_x=\sigma'_3, \varepsilon_y=\varepsilon_x=\varepsilon_3$, and $\varepsilon_z=\varepsilon_1$.

By substituting in equations (A13) and (A12), then

$$k = ½,\ \chi = 1, \text{ and } (\sigma'_1/\sigma'_3) = DKp_\mu \qquad (A14)$$

Equation (A14) is the minimum energy criterion for this case and in agreement with Rowe (1962).

(b) The Case of Plane Strain; $\sigma'_z > \sigma'_y > \sigma'_x$ and $\varepsilon_y = 0$.

$\sigma'_z=\sigma'_1, \sigma'_y=\sigma'_2, \sigma'_x=\sigma'_3$

$\varepsilon_z=\varepsilon_1, \varepsilon_y=\varepsilon_2=0$, and $\varepsilon_x=\varepsilon_3$.

By substituting in equations (A13) and (A12), then

$$k = 1,\ \chi = 1, \text{ and } (\sigma'_1/\sigma'_3) = DKp_\mu \qquad (A15)$$

Rowe (1964) found that the test results did not follow the minimum energy criterion given by Equation (A15); and the agreement was found by replacing Kp_μ by Kp_{cv}, where $Kp_{cv} = \tan^2(45+\phi_{cv}/2)$

(c) The Case of Axial Symmetry, where $\sigma'_z < \sigma'_y = \sigma'_x$.

This is the case of the triaxial extension test. Thus $\sigma'_z=\sigma'_3, \sigma'_y=\sigma'_x=\sigma'_1, \varepsilon_z=\varepsilon_3$, and $\varepsilon_x=\varepsilon_y=\varepsilon_1$.

By substituting in equations (A13) and (A12), then

$$k = ½,\ \chi = 1, \text{ and } (\sigma'_1/\sigma'_3) = (1/D)Kp_\mu \qquad (A16)$$

Equation (A16) is the minimum energy criterion for this case and in agreement with Rowe, Barden and Lee (1964).